P 121

Sub-thrust imaging with a Unified Imaging concept: A Case study from Upper Assam, India

Dasgupta, K.; Reddy, B. J.; Singh, S. N.; *Oil India Limited, Duliajan, India.*
Jaiswal, P.; *Oklahoma State University, Oklahoma, USA.*

Summary

The conventional challenge in depth-imaging – velocity model building with limited aperture seismic survey – becomes more pronounced in fold and thrust belt due to complex geology, inconsistent shot-to-shot energy penetration, and violations of ray-asymptotic assumption. We show that reflection-traveltime inversion and depth migration can be iteratively combined not only to construct geological realistic velocity models but also to test if the constructed velocity model and the corresponding depth-migrated image are "equivalent." The equivalence test allows an interpreter to judge when to stop adjusting or updating the migration velocity model. The application of this combined inversion-migration methods to 2D profiles from Naga Thrust Belt, Assam, India, allows interpretation of a previously unknown triangle zone. The triangle zone appears to be a key in differentiating between successful and dry well targeting sub-thrust traps in the study area and promises future mitigation of drilling risks. This study was performed to build a robust velocity model and depth imaging of seismic data using travel time inversion and pre-stack depth migration methods which will ultimately leads to mapping of key horizons critical for understanding the petroleum geology of sub-thrust in the Upper Assam Shelf in time and depth.

Keywords: *Unified imaging, Velocity-Depth Modeling*

Introduction

It is a common observation that thrust belts deform in a variety of structural style. Presence of multiple décollements, whose location and extent are controlled by stratigraphy, has been attributed as a key factor behind such structural differences. Multiple décollements commonly leads to formation of duplex structures – thrust horses bound by roof and floor detachments overlaying a sequence of cover rocks. Despite an abundance of duplexes and their known potential as hydrocarbon traps, their origin and evolution remains unclear mainly because of a general lack of reliable sub-thrust seismic images.

Conventional depth imaging is a two-step process. The first step is estimation of a background velocity model that describes the large-wavelength characteristics of the subsurface. The second step is imaging of the short-wavelength subsurface features by migration in time or depth with the help of velocity model from the first step. In thrust belts, due to complex ray-paths and high ambient noise, velocity refinement using stacking methods are often interpretation driven. The subjectivity of the process can make the migration velocity model prone to getting biased towards pre-conceived thrust belt models. Further, an incorrect velocity field does not allow seismic energy to be migrated to their correct spatial locations resulting in the images of the reflectors to be improperly focused.

Two wells targeting sub-thrust traps in the Naga Thrust and Fold Belt, Assam, India, meet with very different outcomes – the well drilled near the thrust culmination (W1; Figure 1) is dry while at a similar location 10km to its north-east is producing (W2; Figure 1). Seismic images that were used to guide the drilling were created using conventional processing. These images were unable to explain the difference in the drilling outcome primarily because of their inability to resolve the complexity of structural features expected below the hanging wall. These imaging problems were partly due to the inability of stacking methods in estimate sub-thrust velocities and partly due to the interpreter's inability to judge at what

Geophysics Department, Oil India Limited, Duliajan, Assam-786602
kdgiitr@gmail.com & koustav@oilindia.in

stage should velocity refinements for migration be halted. In this paper we show that traveltime-inversion can be combined with depth-migration to not only develop velocity models that are kinematically correct but also test when to stop updating the migration velocity model. We demonstrate the method with wide-aperture (maximum source-receiver offset ~6km) seismic data.

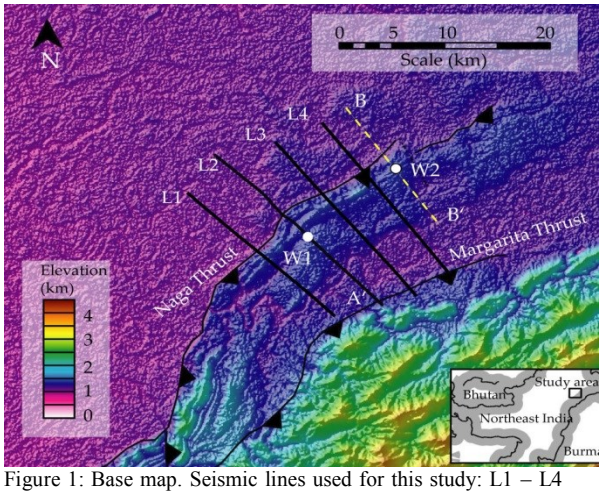

Figure 1: Base map. Seismic lines used for this study: L1 – L4 in solid black line are long-offset data of recent vingate and BB' is narrow-aperture survey of old vintage. Wells, W1 and W2, are shown as white dots. L1 – L4 are imaged using the composite inversion-migration method.

Theory

Imaging steep dips and rapid velocity variations in thrust belts require modeling methods, such as traveltime inversion, that can overcome the hyperbolic ray assumptions inherent in conventional processing. Objective, model-based inversion methods are a reasonable alternative.

A challenge in inversion-based imaging is the solution non-uniqueness which arises due to factors such as inherent non-linearity between data and model parameters, large uncertainties in recording, and inability of numerical methods to address physical realities such as source and receiver directivity. For example, in this paper, imaging is done using reflection arrival-time inversion; the non-linearity arises as velocity model, reflector structure, and ray-paths are all interdependent but unknown at the outset. We have adopted a linearized, gradient-based method which begins with a starting model and updates it iteratively using the difference between the predicted and observed times by minimizing an objective function E:

$$E(s,z) = \delta d^T C_d^{-1} \delta d + \lambda\{\beta[\delta s^T C_{s,h}^{-1} \delta s + s_z \delta s^T C_{s,v}^{-1} \delta s] + (1-\beta)[\delta z^T C_{z,h}^{-1} \delta z]\} \quad (1)$$

In equation (1), $\delta d = d_{pre} - d_{obs}$ are the data errors and $\delta s = s - s_0$ is the slowness (inverse of velocity) perturbation vector being solved for; s_0 is the starting slowness vector, C_d is the data covariance matrix; covariance matrices $C_{s,h}$, and $C_{s,v}$ measure horizontal and vertical roughness of the slowness perturbation, respectively, λ is the trade-off parameter, and s_z determines the relative importance of maintaining vertical versus horizontal model smoothness. $\delta z = z_0 - z$ is the reflector depth perturbation vector; z_0 is the starting reflector vector and $C_{z,h}$ is the covariance matrix that measures the reflector roughness. β determines the relative weights of slowness and reflector regularizations. Substituting $\beta=1$ and $\beta=0$ respectively yields objective functions for travetime only and for reflector only.

While velocity can be updated using ray-based inversion, it is difficult to update the reflector geometry due to issues of relative under-sampling. Therefore, to update the reflector geometry, we adopt migration. Migration, as an overall process of mapping from data to model domain, has led several authors to reformulate it as linearized inversion. Both migration and inversion can be viewed as the reduction of a cost function defined in terms of rock properties, reflectivity in the case of migration and medium contrast in the case of inversion. A similar kinematics thus allows migration and inversion to be coupled using a feedback mechanism (Figure 2) for simultaneously updating velocity as well as reflector geometry.

The ultimate quest, however, is to find out *the stage at which a depth-migrated image can be considered equivalent to the migration velocity model.* Jaiswal and Zelt (2008) argued that with the "true" velocity model, migration and inversion will yield the same structural solution of the geology; they converted a few horizons interpreted in the stacked data to depth (inversion of zero-offset times) and compared to their counterparts in the migrated image using a coefficient and congruence j:

$$j = \frac{1}{n}\sqrt{\sum_{i=1}^{n}\left(\frac{z_i^p - z_i^v}{\sigma_i}\right)^2} \quad (2)$$

In equation (2) z^p and z^v are the interpreted and inverted interfaces and n is the number of nodes at which the interfaces are compared, σ_τ is the interpretation uncertainty at the i^{th} node. A value of unity for $\boldsymbol{j}$ implies that the structural discrepancies have been fit to the level

of the interpretational uncertainties and the unified imaging is said to have converged at this point. Similarly, a value of j greater than unity implies that the velocity model requires improvement and a value less than unity suggests that the data have been overfit. In this paper we follow the Jaiswal and Zelt (2008) imaging method.

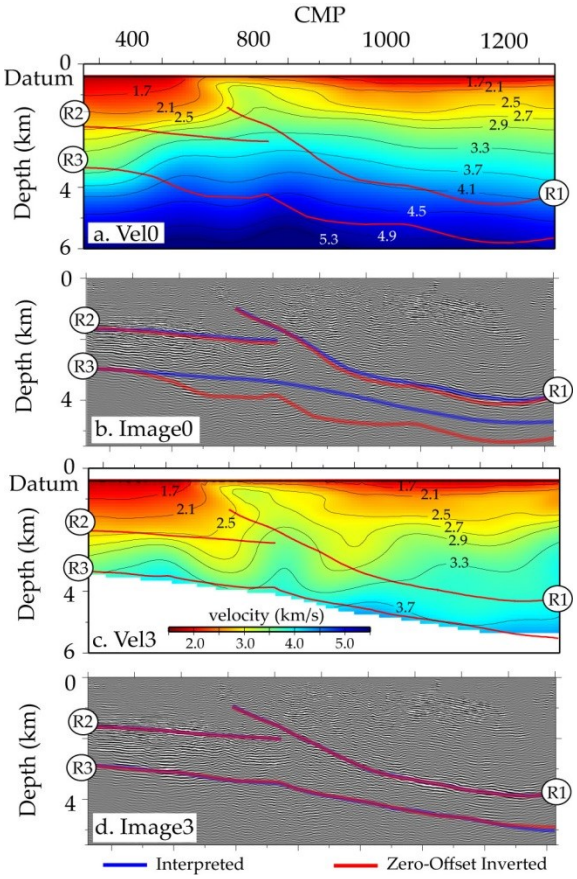

Figure 2: L2 Results. a) Initial model and b) depth imge. c) Final models d) depth image. In a) and c) contours are labeled in km/s. In (a) – (d) geometry of three interfaces, R1 – 3, from inversion of zero-offset (stacked) arrivals are superimposed in red. In c) and d) R1 - 3 interpretations on depth image are in blue. The match in d) indicates convergence to a structural solution.

Application

The seismic data were acquired in the central part of the Upper Assam Shelf perpendicular to the trend of the Naga thrust fault (Figure 1). The variation in topography along all seismic lines is ~70 m. The data were acquired in a split-spread acquisition style with a receiver spacing of 30 m and a nominal fold of 60. The seismic line is ~22 km long and comprises 276 shots fired using Class II explosive sources placed in boreholes typically 30 m deep. The shot spacing ranges form 30–90 m, the minimum offset ranges from 0–30m, and the maximum offset ranges from 5.25–5.43 km. The data were recorded with a sampling interval of 2 ms. Overall the data have a moderate S/N ratio and a broad frequency bandwidth of 8–80 Hz (the background noise has ~30 dB lower power than the signal). In general, the data are contaminated with low frequency, high amplitude ground roll.

Application begins with picking and inversion of first arrivals to generate shallow velocity model which can then be used for static corrections with wave-equation datuming Next, three reflectors that can be consistently identified across the study area are interpreted on all 2D lines (R1 – 3; Figure 2). These reflectors are first picked on stacked data. The velocity model from stacking (e.g. Figure 2a) is then used for scaling them to depth by means of zero-offset inversion ($\beta = 0$; Equation 1). The stacking velocity model is used for depth migration and interpretation of R1 – 3 (Figure 2b). The inverted and interpreted reflectors, R1 – 3, are compared using Equation 2. Simultaneously, wide-aperture picks corresponding to R1 – 3 are made on shot gathers along all the seismic lines. For reflection traveltime inversion of wide-aperture picks to update the velocity model the reflector geometry of R1 – 3 from the current depth image are used. For L3 (Figure 1) the method converges in three iterations yielding a final velocity model (Figure 2c) and a corresponding depth image (Figure 2d).

The application is repeated for individual seismic lines in a similar manner as for L3. For convergence, the method required 4 iterations for L1 data, 3 iterations for L2 data, and 2 iterations for L1 (Figure 3). Stratigraphy along L1 is somewhat more complex that along L4. The number of iterations required for convergence can be thus interpreted as being suggestive not only of the complexity of the velocity model but also its deviation from the stacking velocity that can be obtained by conventional processing.

Interpretation

Based on the reflector geometry and associated velocity structure in Figure 2, the main structural and stratigraphic features can be interpreted. The Naga thrust fault (Feature N, Figure 3) is interpreted between 5-9 km model distance based on the steeply dipping reflectors within CMP 800-1000 based on reflector truncations and within CMP 1000-1250 along the last truncated reflector maintaining a constant thickness; it closely follows the R1 horizon (Figure 2). Surface expression of N is very

well constrained in the Assam Shelf which in turn makes us confident of our interpretation.

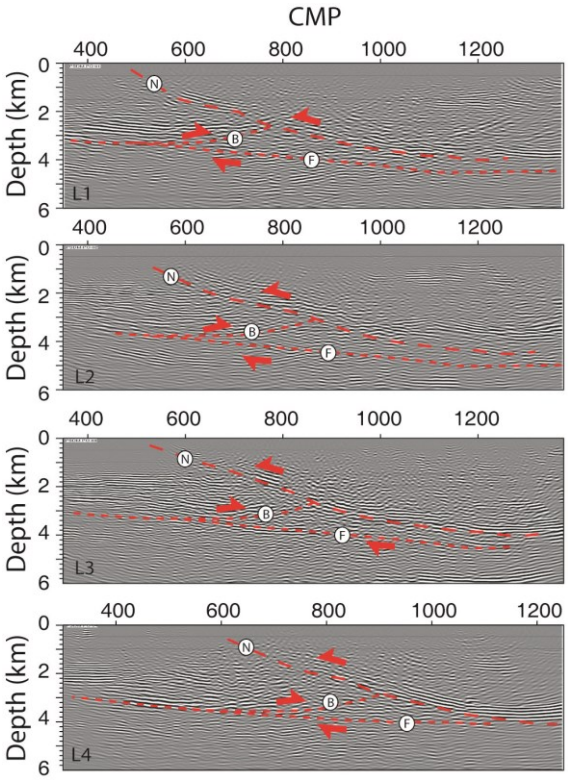

Figure 3: Interpretation. Half-arrows indicate direction of motion. A triangle zone, bounded by three faults, N, F, and B, can be interpreted on all 2D lines.

At 5 km model distance, the reflectors at 3 km depth appear to be diverging in their dips; we interpret the presence of another thrust fault at this location that soles into the foreland stratigraphy within 0-5 km model distance and underlies the northwest dipping stratigraphy in the subthrust (B; Figure 3). The sense of vergence of B is opposite to the Naga thrust fault and it is interpreted as a back-thrust fault to the Naga thrust. The stratigraphy below the Naga thrust fault seems to be expanding toward the back thrust fault. Floor thrust (F; Figure 3) is interpreted at the base of the wedge-shaped stratigraphy. Thrust faults N, B, and F together constitute a triangle zone.

Results

The triangle zone can be interpreted consistently across the seismic lines, L1 – L4, in the study area. As evident in Figure 3, the amplitude of the triangle zone (the maximum height from the floor thrust) appears to be changing in the study area – it is a maximum in L2 and a minimum in L4. At the same time Figure 1 clearly shows that the trace of the Naga thrust Fault is most advanced towards the foreland at L2, i.e., the thrust culmination is along L2. The preceding argument also suggests that the displacements along N and F are inversely related.

The Naga Thrust is the tailing edge of an accretionary prism formed as the Indian plate subducts below the Burmese micro-plate as a result of the mid-Eocene collision of the Indian and the European plates. The "push" from the ongoing subduction can result in a) landward movement of the hanging wall; or b) development of a new-thrust plane. The spatially changing maximum-amplitude of the triangle zone suggests that the displacements with accommodate the ongoing compression in the Naga Thrust and Fold Belt is partitioned between N and F. The back-thrust fault, B, originates probably due to a pre-existing structure in the basement; B and F are a coupled system. The maximum amplitude of the triangle zone, which occurs due to movement along B, is therefore directly proportional to displacement along F. As a result, at the culmination of thrust, e.g., along L2, the maximum displacement occurs along N and the triangle zone is least developed. Conversely, along L4, the maximum displacement occurs along F and the triangle zone is most developed.

We overlay the sonic log of W1 on the depth image of L2. The composite image suggests that W1 penetrates the edge of the triangle zone. Along W2 no data of recent vintage is available. Therefore, we extrapolate the velocity model developed using L1 – L4 and scale profile AA' is depth. We are able to interpret the same triangle zone as in Figure 3 and the overlay of sonic-log from W2 suggests that W2 has penetrated the crest of the triangle zone. Perhaps this explains why W2 produces while W1 is dry. However, more work in terms of imaging, structural restoration, and origin and evolution of the back-thrust fault, is needed to confirm this interpretation.

Conclusion

This paper suggests that a combination of traveltime inversion and PSDM can be a promising approach for depth imaging and interpretation of geological structures in a thrust belt. The method is applied to 2-D multichannel seismic data from the Naga Thrust and Fold Belt, Assam, India. Interpretation of resulting images suggests that displacement partitioning among multiple décollements suggest presence of a duplex structure in the study area deforming through under-thrusting and triangle zone formation. The triangle zone helps in

understanding reasons behind the failure and success of wells in the study area.

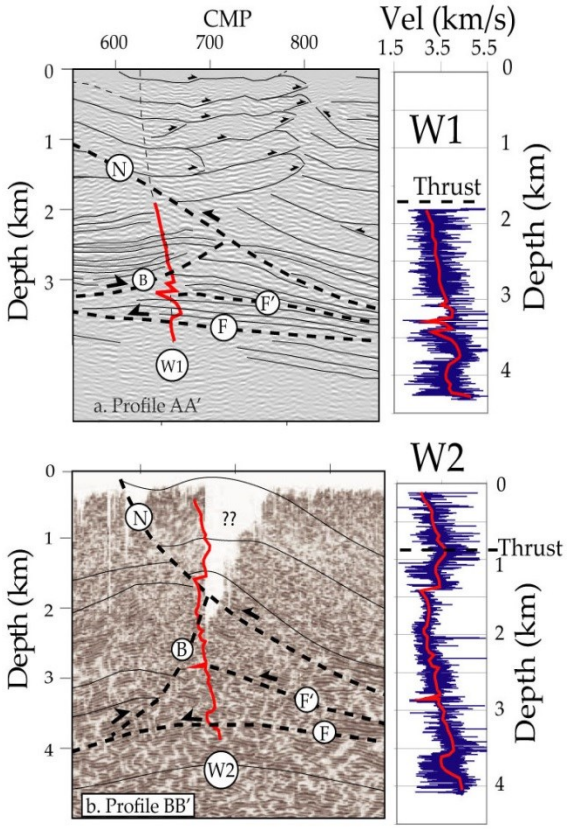

Figure 4: W1 vs W2. W1 does not produce while W2 does. The triangle one interpteted on seismic sections developed using the composite inversion-migrtion method clearly shows that W1 is off-structure. A quasi-3D model of the triangle zone mitigation of drilling risks.

Acknowledgements

The authors sincerely acknowledge Oil India Limited (OIL) for granting permission to publish this paper.

Reference

Jaiswal, P., 2008, Unified imaging of multichannel seismic data: Combining traveltime inversion and prestack depth migration, Geophysics, **73**, 269–280.